



Negative polarization of light at backscattering from a numerical analog of planetary regoliths

Yevgen Grynko^{a,*}, Yuriy Shkuratov^b, Samer Alhaddad^a, Jens Förstner^a

^a Department of Theoretical Electrical Engineering, Paderborn University, Warburger Str. 100, 33102 Paderborn, Germany

^b Institute of Astronomy of Kharkiv National University, Sumska Str. 35, 61022 Kharkiv, Ukraine

ARTICLE INFO

Keywords:

Light backscattering
Linear polarization
Regolith

ABSTRACT

We model negative polarization, which is observed for planetary regoliths at backscattering, solving a full wave problem of light scattering with a numerically exact Discontinuous Galerkin Time Domain (DGTD) method. Pieces of layers with the bulk packing density of particles close to 0.5 are used. The model particles are highly absorbing and have irregular shapes and sizes larger than the wavelength of light. This represents a realistic analog of low-albedo planetary regoliths. Our simulations confirm coherent backscattering mechanism of the origin of negative polarization. We show that angular profiles of polarization are stabilized if the number of particles in a layer piece becomes larger than ten. This allows application of our approach to the negative polarization modeling for planetary regoliths.

1. Introduction

Photopolarimetry is one of the tools that is used in planetary science and remote sensing applications. It allows retrieval of information about physical properties of the surface of a remote object (Videen et al., 2004; Mishchenko et al., 2010; Kolokolova et al., 2015). Solar System bodies like the Moon, Mars, giant planet satellites, asteroids, and cometary nuclei, as well as Kuiper Belt objects are covered with regolith. This is a debris material represented by dust, broken rocks, and glasses, which is a result of long-time meteoroid bombardment. Solar light scattered from such a surface carries information about the structure and composition of the upper layer, which can be extracted from the corresponding Stokes parameters (e.g., Shkuratov et al., 2002; Videen et al., 2004; Shkuratov et al., 2004; Ovcharenko et al., 2006; Shkuratov et al., 2007a; Mishchenko et al., 2010; Kolokolova et al., 2015; Levasseur-Regourd et al., 2015; Nelson et al., 2018; Poch et al., 2018; Muinonen et al., 2015). Potentially, this technique can be used for detection of details on the surfaces of atmosphereless exoplanets as one can assume that similar weathering processes take place in other planetary systems (Wiktorowicz and Stam, 2015).

Photopolarimetric observations of the objects in the Solar System are usually carried at small phase angles, where backscattering optical phenomena, such as the intensity surge (IS) (Shkuratov et al., 2002; Levasseur-Regourd et al., 2015; Ovcharenko et al., 2006; Nelson et al.,

2018;) and the negative polarization (NP) branch, are revealed. These phenomena are quite common for fine-grained surfaces (Lyot, 1929; Shkuratov et al., 1992, 1994; Shkuratov et al., 2002; Shkuratov et al., 2004; Levasseur-Regourd et al., 2015; Ovcharenko et al., 2006; Muinonen et al., 2015). The IS is caused by the shadowing effect, if constituent particles or their aggregates are absorbing, and, partially, by coherent backscattering enhancement (e.g., Shkuratov et al., 2011; Hapke, 2012). The coherent component of IS is a well-known phenomenon not only in remote sensing but in the other fields of optics of discrete media (see e.g., Fazio et al., 2017). The NP branch attracts less interest although it can carry as much information (if not more) about scatterers.

The origin of NP may, in principle, have different mechanisms for samples with different reflectance (Shkuratov et al., 1994, 2011). Single scattering by low-absorbing particles produces strong NP and, therefore, single particles are the main source of NP in densely packed systems with high albedos (Shkuratov et al., 2006; Grynko et al., 2020). Low-albedo surfaces formed by absorbing material also demonstrate noticeable NP feature. Examples are the Moon and dark asteroids (e.g., Shkuratov et al., 1992; Belskaya et al., 2005, 2019) as well as laboratory absorbing powder samples (Shkuratov et al., 2002; Ovcharenko et al., 2006). Highly absorbing single particles that are much larger than the wavelength do not produce NP at backscattering as light scattered from them is mostly reflected from their surface and is always positively

* Corresponding author.

E-mail address: yevgen.grynko@upb.de (Y. Grynko).

<https://doi.org/10.1016/j.icarus.2022.115099>

Received 23 January 2022; Received in revised form 29 April 2022; Accepted 19 May 2022

Available online 23 May 2022

0019-1035/© 2022 Elsevier Inc. All rights reserved.

polarized. At the same time, multiple scattering cannot be significant here due to high absorption and it is limited by the first few orders. Approximate models of double scattering that include interference of conjugate trajectories between pairs of scatterers (Shkuratov, 1985, 1989; Shkuratov et al., 1994; Muinonen, 1989) are able to reproduce NP with reasonable parameters. The effect disappears if this interference is switched off. In such models Fresnel scatterers (Shkuratov, 1985; Shkuratov, 1989), particles with Rayleigh polarization phase functions (Shkuratov, 1991), random distribution of electric dipoles (Muinonen, 1989) or clouds of randomly oriented reflecting facets (Videen, 2002) are considered. Our preliminary simulations show that this mechanism can be non-trivial (Alhaddad et al., 2022), thus, it should be validated for more realistic structures.

An improved model should meet several conditions like dense packing of irregular constituent particles, correct accounting for single-scattering phase function, single-scattering polarization properties of particles and near-field effects that control light transport in a dense medium. This is, however, a complex problem for analytical derivation. It also requires large computational resources due to its multi-scale nature if numerical simulations are applied. This is the reason, why the existing multiple scattering theoretical models are based on various assumptions and approximations which reduces their validity. For instance, models with spherical constituents of very small sizes or samples with low packing densities are often applied for modeling multiple scattering in particulate media (e.g. Ramezanpour and Mackowski, 2019). Light scattering in dense media is also modeled using far-field single scattering characteristics of constituents (Muinonen et al., 2015; Petrova et al., 2019; Kolokolova et al., 2019). Geometrical optics models, that neglect wave effects, can be efficient enough for spectrophotometric applications (e.g., Shkuratov and Grynko, 2005; Schröder et al., 2014) but they fail to reproduce coherent backscattering phenomena. A promising approach is also further development of the T-matrix theory and similar methods that can correctly account for near-field interactions of very close randomly oriented non-spherical particles (Theobald et al., 2017; Markkanen et al., 2018; Bertrand et al., 2020).

Alternatively, a full-wave solution of the problem can be obtained with application of high-performance computing (HPC). This is a resource consuming approach. However, its big advantage is the possibility to consider a realistic target structure. There are no restrictions on the geometry and one can avoid all the assumptions that are inevitably present in approximate models. The input parameters like particle size, complex refractive index and packing density are also in agreement with reality in this case. Thus, determination of their role in the backscattering properties of a densely packed structure becomes straightforward.

In this paper we continue our work on light scattering in dense particulate clusters (Grynko et al., 2020) and apply a numerically exact Discontinuous Galerkin Time Domain (DGTD) method (Hesthaven and Warburton, 2002) and HPC to study the coherent backscattering mechanism of formation of NP. We consider dense systems of absorbing irregular particles that are larger than the wavelength. Owing to high particle absorption one can analyze the roles of single-, and double-scatterings in the formation of NP.

2. Model description

With a numerical model based on the DGTD method and HPC we are able to solve the light scattering problem for a target structure with multi-scale geometry. We consider large dense layers with thickness of a few particles, large monolayers, and small clusters of 2–10 particles lying in one plane. The size parameter ($X = 2\pi r / \lambda$, where r is the radius of the circumscribing sphere and λ is the wavelength) of constituent particles is $X_c = 30$ in all cases. The size parameters of the diameter (D) and thickness (L) of thick layers are $X_D = 200$ and $X_L = 60$, respectively. The number of constituents is $N \approx 150$ in this case. The simplified structures like monolayers of the same diameter contain 50 particles and

the monolayers with the largest diameter $X_D = 250$ consist of 100 particles. Fig. 1a shows examples of a thick layer and a monolayer with 50 particles. The constituent particles in all cases are faceted Gaussian random field shapes (Grynko and Shkuratov, 2003; Grynko and Shkuratov, 2007; Grynko et al., 2018). The complex refractive index of the material is $m = 1.5 + 0.3i$; that is characteristic for amorphous carbon (soot) (Querry, 1985).

Dense packing of irregular constituents is achieved using the *Bullet* physics engine (Coumans and Bai, 2021) which models collisions of arbitrary shapes in time domain. From the initial random sparse distribution of particles in air we simulate their free fall on a substrate under gravity in a closed cylindrical volume. Controlling the number of particles and the size of the cylinder one can generate dense thick granular layers or simple monolayers. The distances between particles in the clusters can be much smaller, comparable to or much larger than the wavelength. This is also a property of real powders consisting of large particles. Consequently, the random variation of heights in the topography of such a layer is also significantly larger than the wavelength which leaves no chance for any noticeable specular reflection.

Then, the densely packed structure is placed in the computational domain and an unstructured mesh required for a DGTD simulation is generated. In all cases we simulate normal incidence of a plane wave along Z axis (Fig. 1b) and calculate far-field scattering matrix elements as functions of the phase angle averaged over azimuth for each sample. A perfectly matched layer (PML) boundary condition is applied to simulate scattering in infinite space.

Fig. 1b shows a cross-section of the computational domain (total field region) with the distribution of the near field intensity $|E|^2$ at steady state. One can see that very little energy penetrates deeper than approximately one particle size. Single scattering and the first few orders of multiple scattering that determine backscattering optical properties take place mostly in the upper layer of particles. Thus, it is impossible to define an elementary scattering volume which is a basic element of the radiative transfer theories (e.g., Hapke, 1981, 2012). This totally excludes application of the classic radiative transfer approach to such media and supports previous critical analysis of the Hapke model (Shkuratov et al., 2012). On the other hand, this an encouraging result for numerical modeling showing that there is no need to use samples with thickness larger than $X_L \approx 50$, at least for this size of constituents and large packing densities. Studying linear polarization requires careful sample averaging, especially in the backscattering range. In all considered cases our results are averaged over the number of samples from 300 to more than 500.

3. Results and discussion

The simulation results for an absorbing thick layer are presented in Fig. 1c and d. Although the thickness of the layer is much smaller than that for laboratory samples the intensity scattering angle curve shows that most of the incident energy is either absorbed or scattered in the back hemisphere. Forward scattering is represented by diffraction and small contribution of external scattering by the particles on the edges of the thick layer (Fig. 1c). In the inset one can see a non-linear dependence of intensity near backscattering caused by coherent enhancement. The linear polarization shows a positive maximum indicating high absorption and low albedo, correspondingly, which is consistent with the Umov effect (Fig. 1d). This is also evidence for low significance of multiple scattering and strong contribution of single scattering at intermediate phase angles. To be more exact, the part of the curve in the phase angle range 90° - 180° is formed mostly by scattering from the sample edges due its finite dimensions and normal illumination. Thus, optical characterization using the Umov law should be done with modeling oblique incidence of light.

At the phase angle of $\approx 12^\circ$ the linear polarization passes inversion point and changes its sign. Here we obtain a negative polarization feature which is qualitatively similar to those measured in experiments

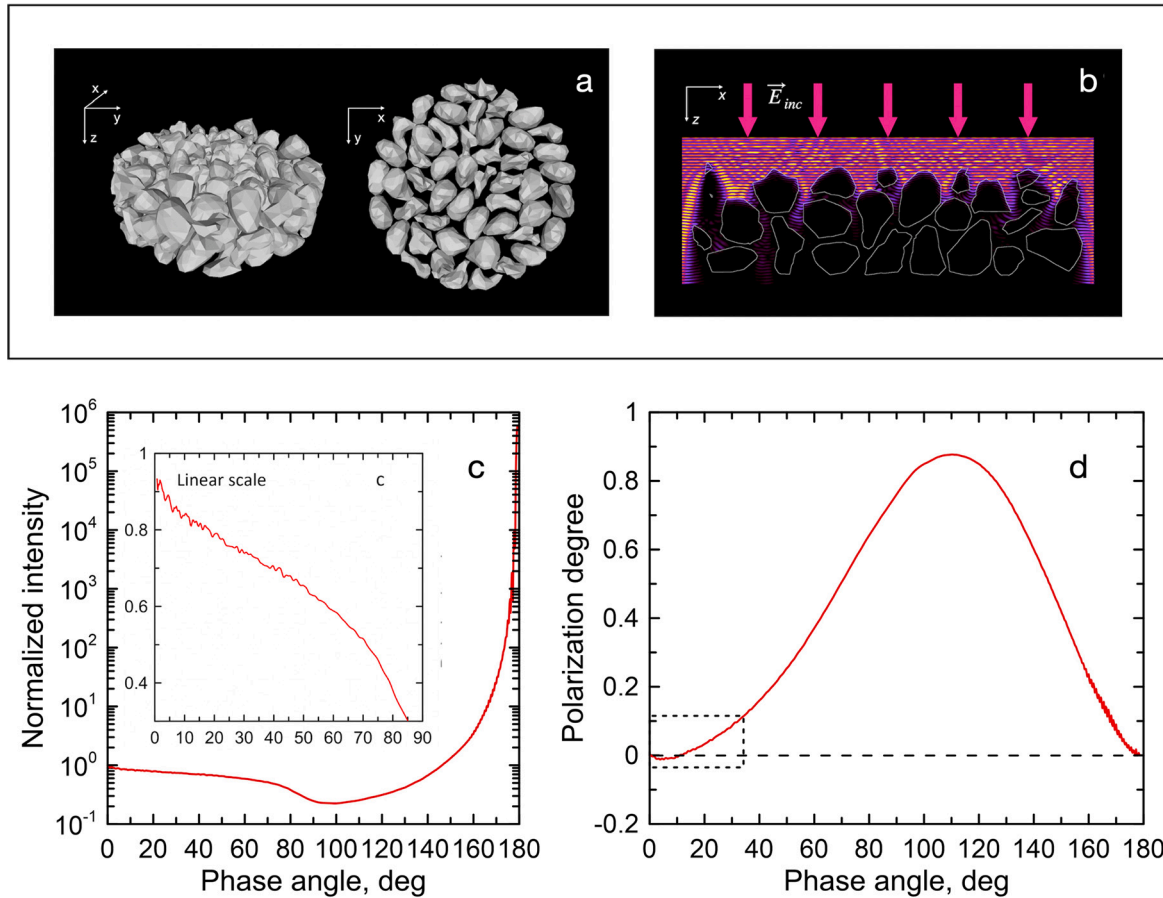


Fig. 1. (a) Examples of a thick particulate layer with diameter $X_D = 200$ and thickness $X_L = 60$ and a monolayer with 50 particles of size $X_c = 30$. (b) Cross-section of the computational domain showing near field intensity ($|E|^2$) distribution at steady state for a thick layer. (c) Phase angle dependencies of intensity in logarithmic and linear scales and the degree of linear polarization (d) computed for dense absorbing thick layers. The diameter and thickness of layers are $X_D = 200$ and $X_L = 60$, respectively. The number of constituents is $N \approx 150$ and the bulk packing density is 0.5.

for soot and low-albedo size-separated samples (e.g., [Ovcharenko et al.,](#)

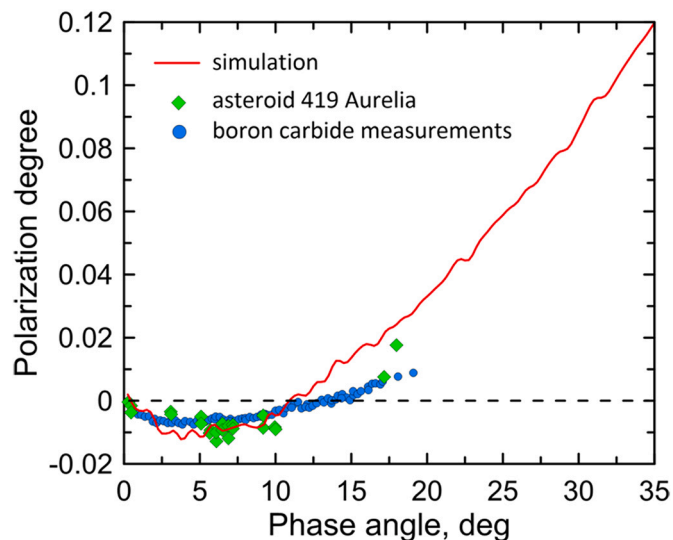


Fig. 2. Comparison of the phase function of linear polarization computed for dense absorbing thick layers and polarimetric measurements of an F-type asteroid 419 Aurelia and a boron carbide powder with particle size $d = 7 \mu\text{m}$. The data is adopted from [Belskaya et al., 2005](#) and [Ovcharenko et al., 2006](#), respectively.

[2006](#)). The result can be compared to the polarimetric data obtained for a dark F-type asteroid 419 Aurelia ([Fig. 2](#)). The corresponding points in [Fig. 2](#) represent V and R band measurements adopted from [Belskaya et al., 2005](#). We also show laboratory data measured by [Ovcharenko et al., 2006](#) for a boron carbide powder. The surface of the sample with the average particle size of $d = 7 \mu\text{m}$ and the wavelength of $\lambda = 0.633 \mu\text{m}$ (size parameter $X_c \approx 35$) is structurally similar to that of our thick layers.

We note that the slope of the positive polarization part of the curve is significantly larger than that for the measurement data. We also estimate the geometrical albedo for our thick layer samples as low as $A = 0.036$. This is similar to the albedos of dark asteroids like 419 Aurelia or 162,173 Ryugu ([Kuroda et al., 2021](#)). The maximum of positive polarization P_{max} does not exceed 60% for such objects (e.g., [Kuroda et al., 2021](#)) as well as for low-albedo laboratory samples ([Shkuratov et al., 2007b](#)). Our result can be explained by the size and morphology of the model particles. All of them are larger than the wavelength and have smooth faceted surface. As a result, single scattering is formed mainly by external reflection producing positive polarization close to Fresnel one. Real particulate surfaces of asteroids and laboratory samples have more complex structure at microscopic scale, and this is the factor reducing the observed P_{max} . In particular, this can be wavelength-scale surface roughness and/or inhomogeneity of large grains, presence of submicron dust stuck to larger particles or small particles that form “fairy castle” structures. An advanced numerical model should include these effects. However, such multi-scale models have not been reported so far due to their complexity.

Considering that the contribution of multiple scattering is

insignificant in our case one can conclude that the backscattering polarization at high absorption is mainly formed by single- and double-scatterings and the NP branch is produced by the coherent double-scattering mechanism suggested in (Shkuratov, 1985; Shkuratov, 1989; Muinonen, 1989). Compact single particles of the above-mentioned size and complex refractive index do not produce NP at all. Their scattering properties are mostly determined by external reflection from their surfaces leading to a Fresnel-like polarization curve. It is very unlikely that orders of scattering higher than three can produce any noticeable contribution for such absorbing particles.

One may anticipate that reducing the particle absorption will increase the effect of higher orders of multiple scattering, which reduces the relative contribution of the first-order scattering. This may lead to increasing the inversion angle. On the other hand, at low absorption individual particles become “sources” of NP even at dense packing (Grynko et al., 2020) and their contribution can be dominating. The inversion angle is determined by the particle size in this case. Moreover, it should be borne in mind that the polarization of high (more than two) orders of scattering gives a significantly smaller contribution to the resulting polarization than the first and second scattering orders. This is because in high scattering orders, light largely “forgets” about its initial polarization and can only produce a depolarization effect.

For better understanding, we simplify the model and consider a monolayer of the same diameter with particles of the same size. In Fig. 3a and b we compare the intensity and linear polarization results for thick layers and monolayers. Polarization curves confirm our conclusion. In a monolayer multiple scattering is naturally limited by the

geometry but the polarization backscattering response appears to be similar to that from a thick layer. This means that the NP feature is formed by the relatively simple process of scattering between particles in the very upper layer. Interestingly, there is a big difference in the intensity curves. A monolayer shows an almost flat angular dependency with a peak caused by coherent backscattering enhancement. The thick layer structure shows a curve apparently formed by the shadowing effect with monotonous decrease of reflectance in the entire range of 0–80°. This also partially obscures coherent backscattering intensity peak.

It is reasonable to reduce the system down to the simplest case of just two and four particles with minimum distance between them. In Fig. 3c we compare the computed linear polarization at backscattering for single particles and small structures of a few particles lying in one plane. Single scattering by isolated absorbing particles of this kind does not show any NP. A two-particle system reveals a small but well detected NP feature which proves the coherent double-scattering mechanism. The feature gets enhanced with increasing number of particles. This can be explained by the increasing relative contribution of double scattering with respect to single one. In two-particle samples there is only one possibility for double scattering and there are two scatterers that are “sources” of single scattering that does not contribute to NP. With four different particles lying in one plane the number of neighbors and, correspondingly double scattering paths is 6 which increases the probability of the coherent backscattering enhancement. However, single scattering from the edges of such a structure still can be large. The enhancement continues to the number of ten, and one can assume that the results start converging at this. Indeed, simulations for larger

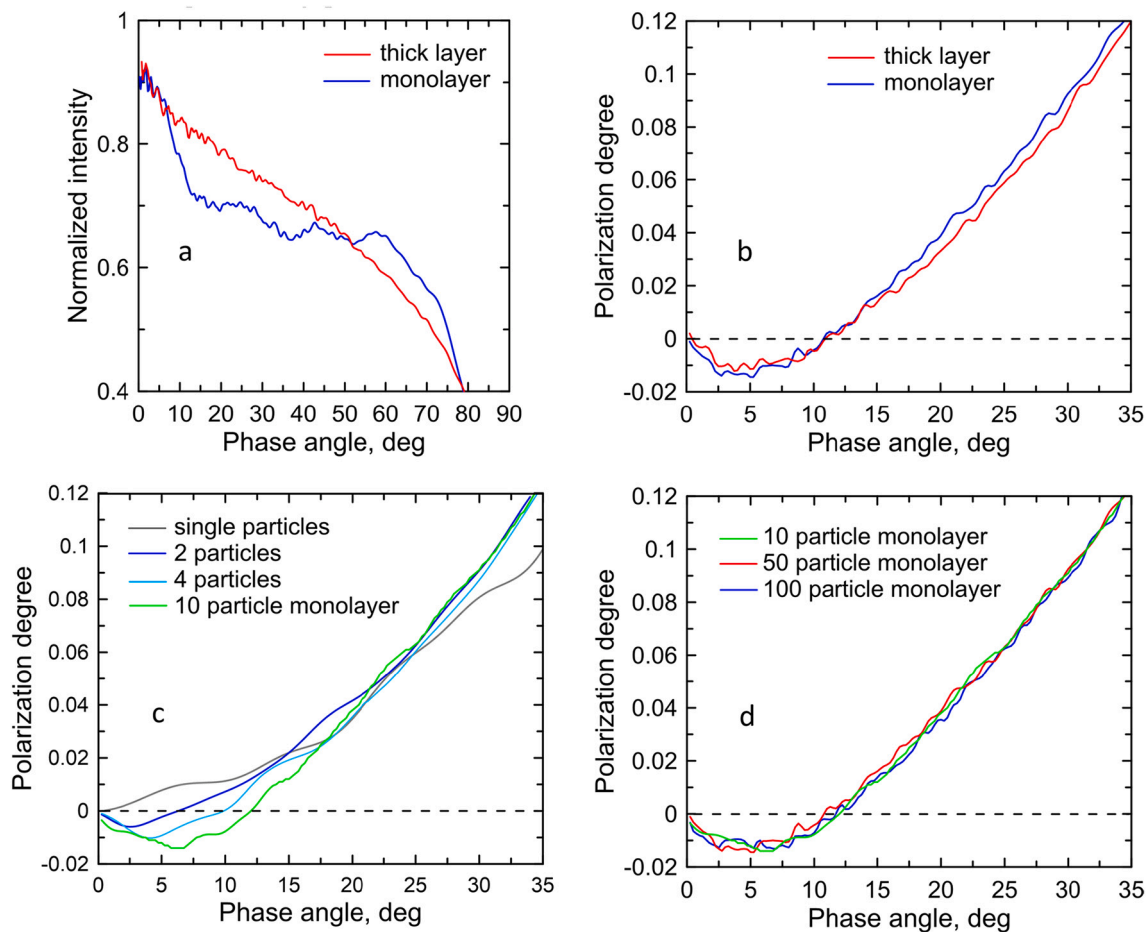


Fig. 3. Phase angle dependencies of intensity (a) and degree of linear polarization (b) computed for thick layer and monolayer samples with the same diameters ($X_D = 200$). Comparison of the degree of linear polarization at backscattering computed for single particles, 2-, 4- and 10-particle structures (c) and monolayers of 50 ($X_D = 200$) and 100 particles ($X_D = 250$) (d).

systems, monolayers with 50 and 100 particles (the diameter of the sample is $X_D = 250$ in the last case), show that polarization does not change significantly anymore (Fig. 3d). This means that single scattering from the edges makes negligible contribution to backscattering. Thus, for backscattering simulations and highly absorbing materials, one should consider structures with at least ten or a few tens of constituents on the surface. Below this number the result may depend on the size of the system. We note that shadowing effect plays minor role here. However, it should be taken into account for correct intensity computations which is possible in thick layers only.

4. Conclusion

Numerically exact full-wave solution for various systems of densely packed absorbing irregular particles, thick layers and monolayers, shows that the polarization backscattering response is mainly a result of single- and double-scattering in the upper layer of a particulate structure and the NP effect is produced by coherent double-scattering. At high packing density an absorbing layer with thickness of a few particle sizes (if the particles are larger than the wavelength) can already be optically thick. Thus, there is no need to consider very thick layers in such numerical simulations. The angular dependence of linear polarization at backscattering converges if the number of particles on the surface is larger than ten. With this we specify a lower limit for the number of constituents in the numerical studies of NP of light scattered from absorbing particulate layers. Our results show that any definition of an elementary scattering volume, which is a crucial element of the radiative transfer theories describing multiple scattering, is not feasible in the considered particulate structures. This totally excludes application of the radiative transfer approach to such media.

Declaration of Competing Interest

None.

Acknowledgment

The authors gratefully acknowledge the computing time granted by the Paderborn Center for Parallel Computing (PC²) and by the John von Neumann Institute for Computing (NIC) on the supercomputer JURECA at Jülich Supercomputing Centre (JSC).

References

- Alhaddad, S., Grynko, Y., Farheen, H., Förstner, J., 2022. Numerical analysis of the coherent mechanism producing negative polarization at backscattering from systems of absorbing particles. *Opt. Lett.* 47, 58–61.
- Belskaya, I.N., Shkuratov, Yu.G., Efimov, Yu.S., Shakhovskoy, N.M., Gil-Hutton, R., Cellino, A., Zubko, E.S., Ovcharenko, A.A., Bondarenko, S.Yu., Shevchenko, V.G., Fornasier, S., Barbieri, C., 2005. The F-type asteroids with small inversion angles of polarization. *Icarus* 178, 213–221.
- Belskaya, I., Cellino, A., Levasseur-Regourd, A.-C., Bagnulo, S., 2019. Optical polarimetry of small solar system bodies: from asteroids to debris disks. In: Mignani, R., Shearer, A., Stowikowska, A., Zane, S. (Eds.), *Astronomical Polarisation from the Infrared to Gamma Rays*, Astrophysics and Space Science Library, vol. 460. Springer, Cham, pp. 223–246.
- Bertrand, M., Devilez, A., Hugonin, J.P., Lalanne, P., Vynck, K., 2020. Global polarizability matrix method for efficient modeling of light scattering by dense ensembles of non-spherical particles in stratified media. *J. Opt. Soc. Am. A* 37, 70–83.
- Coumans, E., Bai, Y., 2021. Pybullet, A Python Module for Physics Simulation for Games, Robotics and Machine Learning. <http://pybullet.org>.
- Fazio, B., Irrera, A., Pirota, S., D'Andrea, C., Del Sorbo, S., Faro, M.J.L., Gucciardi, P.G., Iati, M., Saija, R., Patrini, M., Musumeci, P., Vasi, C.S., Wiersma, D.S., Galli, M., Priolo, F., 2017. Coherent backscattering of raman light. *Nat. Photonics* 11, 170–176.
- Grynko, Y., Shkuratov, Y., 2003. Scattering matrix calculated in geometric optics approximation for semitransparent particles faceted with various shapes. *J. Quant. Spectrosc. Radiat. Transf.* 78, 319–340.
- Grynko, Y., Shkuratov, Y., 2007. Ray tracing simulation of light scattering by spherical clusters consisting of particles with different shapes. *J. Quant. Spectrosc. Radiat. Transf.* 106, 56–62.
- Grynko, Y., Shkuratov, Y., Förstner, J., 2018. Intensity surge and negative polarization of light from compact irregular particles. *Opt. Lett.* 43, 3562–3565.
- Grynko, Y., Shkuratov, Y., Förstner, J., 2020. Light backscattering from large clusters of densely packed irregular particles. *J. Quant. Spectrosc. Radiat. Transf.* 255, 107234.
- Hapke, B., 1981. Bidirectional reflectance spectroscopy. I. Theory. *J. Geophys. Res.* 86, 3039–3054.
- Hapke, B., 2012. *Theory of Reflectance and Emittance Spectroscopy*. Cambridge Univ. Press, Cambridge, p. 513.
- Hesthaven, J.S., Warburton, T., 2002. Nodal high-order methods on unstructured grids: I. time-domain solution of maxwell's equations. *J. Comput. Phys.* 181, 186–221.
- Kolokolova, L., Hough, J., Levasseur-Regourd, A.-C., 2015. *Polarimetry of Stars and Planetary Systems*. Cambridge University Press.
- Kolokolova, L., Ito, G., Pitman, K.M., McMichael, K., Reui, N., 2019. Spectral modeling using radiative transfer theory with packing density correction: demonstration for Saturnian icy satellites. *Planet. Sci. J.* 1, 74.
- Kuroda, D., Geem, J., Akitaya, H., Jin, S., Takahashi, J., Takahashi, K., Naito, H., Makino, K., Sekiguchi, T., Bach, Y.P., Seo, J., Sato, S., Sasago, H., Kawabata, K.S., Kawakami, A., Tozuka, M., Watanabe, M., Takagi, S., Kuramoto, K., Yoshikawa, M., Hasegawa, S., Ishiguro, M., 2021. Implications of high polarization degree for the surface state of Ryugu. *Astrophys. J. Lett.* 911, L24.
- Levasseur-Regourd, A.-C., Renard, J.-B., Shkuratov, Y., Hadamcik, E., 2015. Laboratory studies. In: Kolokolova, L., Hough, J., Levasseur-Regourd, A.-C. (Eds.), *Polarimetry of Stars of Stars and Planetary Systems*. Cambridge University Press, pp. 62–80.
- Lyot, B., 1929. Recherches sur la polarisation de la lumière des planètes et de quelques substances terrestres. *Ann. Obs. Meudon.* 8 (1), 1–161.
- Markkanen, J., Väisänen, T., Penttilä, A., Muinonen, K., 2018. Scattering and absorption in dense discrete random media of irregular particles. *Opt. Lett.* 43, 2925–2928.
- Mishchenko, M., Rosenbush, V., Kiselev, N., Lupishko, D., Tishkovets, T., Kaydash, V., Belskaya, I., Efimov, Y., Shakhovskoy, N., 2010. *Polarimetric Remote Sensing of Solar System Objects*. Akademiya Nauk, Kiev, p. 291.
- Muinonen, K., 1989. Electromagnetic scattering by two interacting dipoles. In: *Proc. 1989 URSI Electromagn. Theory Symp.* Stockholm, Sweden, pp. 428–430.
- Muinonen, K., Penttilä, A., Videen, G., 2015. Multiple scattering of light in particulate planetary media. In: Kolokolova, L., Hough, J., Levasseur-Regourd, A.-C. (Eds.), *Polarimetry of Stars and Planetary Systems*. Cambridge University Press, pp. 114–129.
- Nelson, R.M., Boryta, M.D., Hapke, B.W., Manatt, K.S., Shkuratov, Y., Psarev, V., Vandervoort, K., Kroner, D., Nebedum, A., Vides, C.L., Quinones, J., 2018. Laboratory simulations of planetary surfaces: understanding regolith physical properties from remote photopolarimetric observations. *Icarus* 302, 483–498.
- Ovcharenko, A.A., Bondarenko, S.Y., Zubko, E.S., Shkuratov, Y.G., Videen, G., Nelson, R. M., Smythe, W.D., 2006. Particle size effect on the opposition spike and negative polarization. *J. Quant. Spectrosc. Radiat. Transf.* 101, 394–403.
- Petrova, E.V., Tishkovets, V.P., Nelson, R.M., Boryta, M.D., 2019. Prospects for estimating the properties of a loose surface from the phase profiles of polarization and intensity of the scattered light. *Sol. Syst. Res.* 53, 172–180.
- Poch, O., Cerubini, R., Pommerol, A., Jost, B., Thomas, N., 2018. Polarimetry of water ice particles providing insights on grain size and degree of sintering on icy planetary surfaces. *J. Geophys. Res. Planets* 123, 2564–2584.
- Querry, M.R., 1985. Optical constants. In: *Contractor Report CRDC-CR-85034*.
- Ramezanpour, B., Mackowski, D.W., 2019. Direct prediction of bidirectional reflectance by dense particulate deposits. *J. Quant. Spectrosc. Radiat. Transf.* 224, 537–549.
- Schröder, S.E., Grynko, Y., Pommerol, A., Keller, H.U., Thomas, N., Roush, T.L., 2014. Laboratory observations and simulations of phase reddening. *Icarus* 239, 201–216.
- Shkuratov, Y.G., 1985. On the opposition brightness surge and light negative polarization of solid cosmic surfaces. *Astron. Circ.* 1400, 3–6 (in Russian).
- Shkuratov, Y., 1989. Interference mechanism of opposition spike and negative polarization of atmosphereless planetary bodies. *Bull. Am. Astron. Soc.* 21, 989.
- Shkuratov, Y.G., 1991. An interference model of the negative polarization of light scattered by atmosphereless celestial bodies. *Sol. Syst. Res.* 25, 134–142.
- Shkuratov, Y., Grynko, Y., 2005. Light scattering by media composed of semitransparent particles of different shapes in ray optics approximation: consequences for spectroscopy, photometry, and polarimetry of planetary regoliths. *Icarus* 173, 16–28.
- Shkuratov, Y., Opanasenko, N., Kreslavsky, M., 1992. Polarimetric and photometric properties of the moon: telescopic observations and laboratory simulations: 1. The negative polarization. *Icarus* 95, 283–299.
- Shkuratov, Y.G., Muinonen, K., Bowell, E., Lumme, K., Peltoniemi, J., Kreslavsky, M.A., Stankevich, D.G., Tishkovets, V.P., Opanasenko, N.V., Melkumova, L.Ya., 1994. A critical review of theoretical models for the negative polarization of light scattered by atmosphereless solar system bodies. *Earth Moon Planet.* 65 (3), 201–246.
- Shkuratov, Y., Ovcharenko, A., Zubko, E., Miloslavskaya, O., Muinonen, K., Piironen, J., Nelson, R., Smythe, W., Rosenbush, V., Helfenstein, P., 2002. The opposition effect and negative polarization of structural analogs for planetary regoliths. *Icarus* 159, 396–416.
- Shkuratov, Y., Videen, G., Kreslavsky, M., Belskaya, I., Kaydash, V., Omelchenko, V., Opanasenko, N., Zubko, E., 2004. Scattering properties of planetary regoliths near opposition. In: Videen, G., Yatskiv, Y., Mishchenko, M. (Eds.), *Photopolarimetry in Remote Sensing*. Springer, Netherlands, pp. 191–208.
- Shkuratov, Y., Bondarenko, S., Ovcharenko, A., Pieters, C., Hiroi, T., Volten, H., Munoz, O., Videen, G., 2006. Comparative studies of the reflectance and degree of linear polarization of particulate surfaces and independently scattering particles. *Quant. Spectrosc. Radiat. Transf.* 100, 340–358.
- Shkuratov, Y., Opanasenko, N., Zubko, E., Grynko, Y., Korokhin, V., Pieters, C., 2007a. Multispectral polarimetry as a tool to investigate texture and chemistry of lunar regolith particles. *Icarus* 187, 406–416.

- Shkuratov, Y., Bondarenko, S., Kaydash, V., Videen, G., Volten, H., Munoz, O., 2007b. Photometry and polarimetry of particulate surfaces and aerosol particles over a wide range of phase angles. *Quant. Spectrosc. Radiat. Transf.* 106, 487–508.
- Shkuratov, Y., Kaydash, V., Korokhin, V., Velikodsky, Y., Opanasenko, N., Videen, G., 2011. Optical measurements of the moon as a tool to study its surface. *Planet. Space Sci.* 59, 1326–1371.
- Shkuratov, Y., Kaydash, V., Korokhin, V., Velikodsky, Petrov, Zubko, E., Stankevich, D., Videen, G., 2012. A critical assessment of the Hapke photometric model. *Quant. Spectrosc. Radiat. Transf.* 113, 2431–2456.
- Theobald, D., Egel, A., Gomard, G., Lemmer, U., 2017. Plane-wave coupling formalism for T-matrix simulations of light scattering by nonspherical particles. *Phys. Rev. A* 96, 033822.
- Videen, G., 2002. Polarization opposition effect and second-order ray tracing. *Appl. Opt.* 41, 5115–5121.
- Videen, G., Yatskiv, Y., Mishchenko, M., 2004. *Photopolarimetry in Remote Sensing*. Kluwer Academic Publishers.
- Wiktorowicz, S.J., Stam, D.M., 2015. Exoplanets. In: Kolokolova, L., Hough, J., Levasseur-Regourd, A.-C. (Eds.), *Polarimetry of Stars of Stars and Planetary Systems*. Cambridge University Press, pp. 439–461.